Dynamic modelling of a non conventional thrust-vectored airship

DYNAMIC MODELLING OF A NON CONVENTIONAL THRUST-VECTORED AIRSHIP

M. Battipede[*], P.A. Gili[+], L. Massotti[+], P. Vercesi[‡]
[*] *Department of Mechanics, Polytechnic of Turin, 10129 Turin, Italy*
[+] *Department of Aeronautical and Space Engineering*
Polytechnic of Turin, 10129 Turin, Italy
[‡] Nautilus S.r.l. – Alessandria, ITALY

ABSTRACT

This paper is concerned with a simulation tool developed for the innovative lighter-than-air airship patented by Nautilus S.r.l. This unmanned airship does not use aerodynamic control surfaces: the primary command system consists in a set of propellers properly placed in order to control and maneuver the airship within the whole flight envelope. Control strategies are different for the two possible flight situations: hovering and forward flight. The simulation package is modular and flexible so that different levels of modelling can be accomplished implementing various airship models, aerodynamic database and control procedures. Flight tests performed on the flight simulator point out that the airship is sufficiently maneuverable even if in a open-loop configuration, namely without automatic control devices.

List of Acronyms

CAS	Control Augmentation System
CB	Center of Buoyancy
CG	Center of Gravity
CV	Center of Volume
DOF	Degree Of Freedom
FFD	Fan Front Down
FFU	Fan Front Up
FRD	Fan Rear Down
FRU	Fan Rear Up
FTI	Flight Instrumentation System
FVA	Fan Vertical Aft
FVF	Fan Vertical Fore
LTA	Lighter Than Air
RPM	Revolutions Per Minute
SAS	Stability Augmentation System
VTOL	Vertical Take Off and Landing

List of Symbols

B	Buoyancy
C_{F_x,F_y,F_z}	Force coefficients
$C_{L,M,N}$	Moment coefficients
D	Hull diameter
F_X, F_Y, F_Z	Total forces
I_x, I_y, I_z	Main inertia moments
I_{xy}, I_{xz}, I_{yz}	Products of inertia
J_x, J_y, J_z	Apparent main inertia moments
J_{xy}, J_{xz}, J_{yz}	Apparent products of inertia
L	Roll moment
$\overset{\circ}{L}_{\dot{p}}, \overset{\circ}{M}_{\dot{q}}, \overset{\circ}{N}_{\dot{r}}$	Gas main inertia
$\overset{\circ}{L}_{\dot{q}}, \overset{\circ}{N}_{\dot{p}}, \overset{\circ}{M}_{\dot{r}}$	Gas products of inertia
$\overset{\circ}{M}_{\dot{p}}, \overset{\circ}{L}_{\dot{r}}, \overset{\circ}{N}_{\dot{q}}$	
M	Pitch moment
N	Yaw moment
R	Propeller radius
T	Thrust
T_K	Absolute temperature
U	Free-stream airspeed
V	Volume of hulls
X,Y,Z	CG reference frame
$\overset{\circ}{X}_{\dot{u}}, \overset{\circ}{Y}_{\dot{v}}, \overset{\circ}{Z}_{\dot{w}}$	Gas masses
b_x, b_z	Coordinates of CB
g	Gravity acceleration
l	Reference length of the wet surface
m	Mass
m_x, m_x, m_x	Apparent masses
p	Roll angular rate
p_a	Atmospheric pressure
$\dot{p}$	Roll angular acceleration
q	Pitch angular rate
$\dot{q}$	Pitch angular acceleration
r	Yaw angular rate
$\dot{r}$	Yaw angular acceleration
u, v, w	Components of translation velocity
$\dot{u}, \dot{v}, \dot{w}$	Components of translation acceleration
α	Angle of attack
β	Sideslip angle
ε	Ratio of specific weights
φ, ϑ, ψ	Euler angles
ρ	Density

ω	Pulsation
Λ	Specific weight

Subscripts

He	Helium
K	Kelvin
a	aerodynamic
air	air
b	buoyancy
e	trim
fw	forward
g	gravitational
lat	lateral
lon	longitudinal
or	oscillatory roll mode
pr	propulsion
p, q, r	angular rates
ph	phugoid
s	sideslip subsidence mode
sp	short period
u ,v ,w	linear velocity
vt	vertical
y	yaw subsidence mode

1. Introduction

Even if airships represent a small fraction of the aerospace market, in the last decade the interest on unmanned aerial vehicles has grown for both commercial and military applications. As a matter of fact, remotely-piloted airships represent the most interesting vehicle for low speed, low altitude exploration and monitoring missions. In virtue of the aerostatic lift they are noiseless, non-obtrusive, ecological and useful for environmental applications[1], such as oceanographic[2-3] and agricoltural studies, traffic monitoring, ecological and climate research, inspection of endangered ecological sites as well as long-term variability studies. In addition, they have already proved themselves useful as camera and TV platforms as well for specialised scientific tasks.

The LTA vehicles present some advantages over other transports in civil applications[4]: especially without airport facilities, some places are accessible only by the hovering capability of airships and helycopters. Actually, airship can operate as a rotary-wing aircraft but it benefits from the absence of rotors, which generally imply high structural design costs and strong payload (cameras and monitoring equipments) vibrations. As drawback, the most crucial aspect of the conventional airship handling is its poor capability of operating in adverse environmental conditions. This is due to the features of the conventional primary command system, together with the low weight and the big size of the whole body. In fact, aerodynamic surfaces are poorly efficient as they are generally covered by the separate stream of the hulls[5]. Moreover, in low and moderate speeds, the aerodynamic surface deflections must be very large getting very close to the stall conditions even for standard maneuvers and light gusts.

In order to improve maneuverability and enlarge the conventional airship flight envelope, with a special concern in the VTOL and hovering capabilities both in normal and severe wind conditions, an innovative lighter-than-air platform is designed and patented by Nautilus S.r.l., featuring an architecture and an *ad-hoc* command system to overcome the problems discussed above.

This paper is focused on the modelling phase of the Nautilus new concept unmanned airship. In this context, the modelling phase represents an intermediate step between the design and the final manufacturing of the airship and its control system. The airship mathematical model is based on a 6 DOF nonlinear model[6,7] implemented in a graphical software environment within Matlab/Simulink which simplifies the validation of control and navigation strategies.

To display and evaluate the pilot interaction, the dynamic model is interfaced with a visual simulation software and is flown through a joystick. An innovative cockpit design is also being developed to cope with the unconventional command system. As this matter seems to be crucial, modelling is fundamental to implement several cockpit options. This should allows to select the best solution to satisfy the standard aviation regulations, which require that a standard skilled pilot might learn to fly the vehicle without too demanding training sections.

Examples of maneuvers are provided together with a stability analysis of the airship dynamic characteristics.

2. Airship Characteristics

The Nautilus unmanned airship (Figure 1) features a double hull architecture with a central plane housing structure and propellers. Lift is provided by a hybrid system consisting in helium for the aerostatic lift and a system of vertical axis propellers which supplies the vertical thrust for climb and descent maneuvers. In forward flight buoyancy is also enforced by the aerodynamic lift of the whole body.

As it can be seen in Figure 1, the unmanned airship does not use aerodynamic control surfaces. The primary command system consists in six propellers properly set to obtain a system of forces and moments, suitable to control and maneuver the airship in its flight envelope with a lateral wind up to 15 knots. All the propellers are moved by electrical motors feeded with an on-board generation system. Two of them have already been mentioned as the vertical axis propellers

used to provide vertical thrust. Moreover, they also contribute to control the pitch attitude of the airship by differential fore and aft rotational speed. The other four propellers are mounted on vertical arms, disposed at a proper distance from the whole body Center of Gravity (CG): the arms rotation, together with the variation of the propellers rotational speed, should allow to vary the direction and the absolute value of the thrust. As a consequence the airship can be properly maneuvered in pitch, roll and yaw angular rates.

In order to handle altitude variations without losing helium from the hulls, the airship is equipped with ballonets (one for each hull) which are controlled through an *ad-hoc* pneumatic system consisting in pipes and valves. Ballonets are communicant as well as the gas volume of the hulls. During the climb, initially the air is released from ballonets and then, if the altitude increases overtaking the *plenitude altitude* (namely the altitude to which the gas is completely expanded filling the hulls), the helium is also released from hulls. During the descent, ballonets are blown up using a dynamic intake and a compressor. In this way the air and gas centers of volume are kept approximately in a fixed hull section: consequently, the aerostatic lift center is higher than the Center of Gravity improving the airship lateral stability.

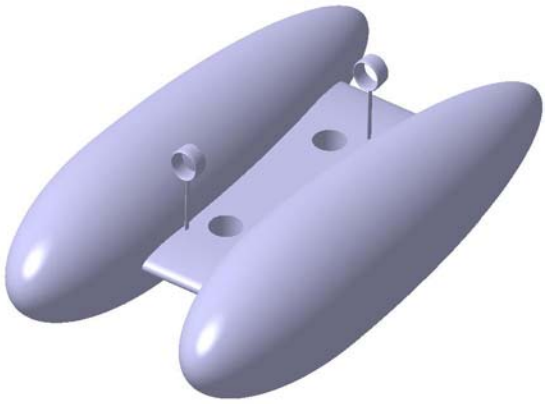

Figure 1. The Nautilus new concept unmanned airship

3. Control System

As it can be seen in Figure 2, the primary command system is a based on six propellers properly set along the central plane of the airship.

In order to build a flight simulator as accurate as possible, an hardware version of the control system has been accomplished and linked to the Simulink environment. It consists of two throttles and a joystick with a manual switch, futhermore control strategies are different for the two possible flight situations: hovering and forward flight. The switch enable to change manually strategy according to what is more convenient in the current flight condition. In both cases, the first throttle equally varies the RPM of the four forward propellers at the same time, while the second one controls the RPM of the two vertical axis propellers.

According to the desired flight condition, the pilot has the possibility to accomplish different control laws through the three DOF of the joystick. As a matter of fact, in forward flight the rotation around the vertical axis generates a yaw moment through the differential turn of the thrust axes of front and rear engines. The lateral shift of the stick causes a differential rotation of the thrust axes of the upper and lower engines, generating a roll moment. Finally, the longitudinal command produces a differential variation of the RPM of horizontal and vertical axis propellers generating a differential thrust and consequently a pitch moment.

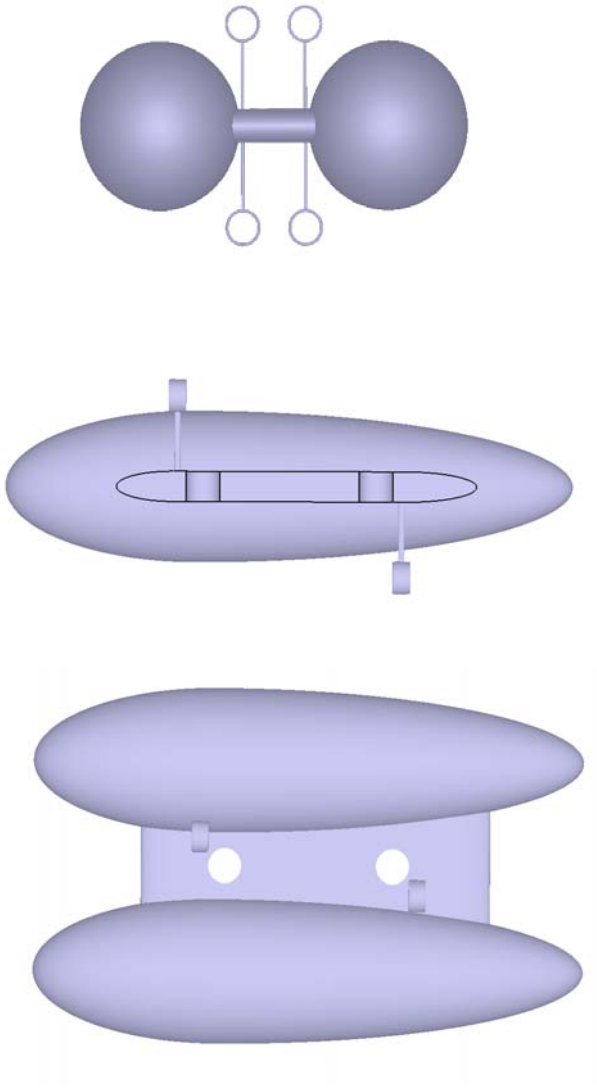

Figure 2. Airship triptych

On the other hand, in the hovering control strategy, the rotation around the joystick vertical axis commands the turn rate of the thrust axes of the forward propellers. In this way they are turned in the same direction according to the wind direction that must be opposed, and their rotations depend on the amount of joystick whirl and duration of the command impulse. The longitudinal command of the stick causes a differential thrust as in the forward flight condition, while the stick lateral shift generates a yaw moment through the right and left differential thrust of the propellers in order to orient the airship in the desired aft.

The airship is equipped with Control Augmentation Systems (CAS) featuring autopilot capabilities to keep the steady-state flight conditions and follow specific flight-paths[8]. In addition, due to the longitudinal and lateral intrinsic instability of the fuse architecture, a Stability Augmentation System (SAS) has to be designed to achieve the desired dynamic characteristics. Autopilot systems such as wing level, altitude hold and heading hold must be installed as well on board in order to guarantee comfortable flying qualities. At this purpose the airship is fitted out with a considerable number of sensors to measure flight parameters not only for the definition of the Flight Test Instrumentation (FTI) system but also to provide feedback signals to automatic control systems[9] mentioned above.

4. Mathematical Model

The airship mathematical model is based on a 6 DOF nonlinear model that follows the standard conventional aircraft dynamic modeling but differs from it for the following considerations:
- the airship is buoyant and displaces a large volume, therefore the buoyancy force *B* and apparent mass and inertia terms are significant additions to the familiar aircraft equations of motion;
- due to the constantly changing Center of Gravity (CG) position, the airship motion is usually referenced to a system of orthogonal body axes fixed in the vehicle with the origin at the Center of Volume (CV) that is assumed to coincide with the gross Center of Buoyancy (CB). However, in this paper the formulation of the equations of motion has been carried out referring the total forces and moments to the airship CG, since the CG and CB positions with respect to a body-fixed reference frame are known at each time step of simulation.

The airship CG coordinate system is shown in Figure 3 with the total forces (F_X, F_Y, F_Z) and moments (L, M, N) around the X, Y, and Z axes respectively. The orientation of this reference frame with respect to an Earth-fixed system is obtained through the Euler angles φ, ϑ and ψ.

In building this mathematical model only two limiting assumptions have been made:
- the airship is treated as a rigid body without aeroelastic effects;
- the vehicle is symmetric about the XZ plane such that both the CV and the CG lie in the plane of symmetry.

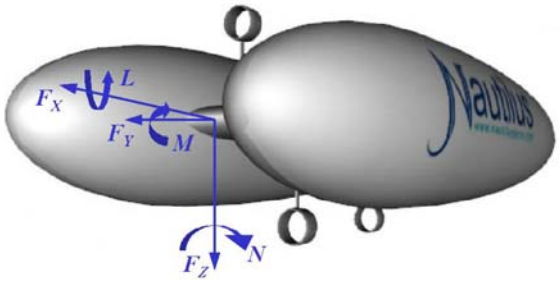

Figure 3. Force and moments acting on the airship

The gas mass and inertia effects[5] are described by the dimensional derivatives of aerodynamic force and moment with respect to linear ($\dot{u}, \dot{v}, \dot{w}$) and angular ($\dot{p}, \dot{q}, \dot{r}$) acceleration perturbations. These terms are assessed through the CAD program *Catia* and are simply added to the physical mass *m* and inertia terms *I* in the development of the equations of motion. The components of apparent mass are expressed as follows:

$$m_x = m - \overset{\circ}{X}_{\dot{u}} \qquad m_y = m - \overset{\circ}{Y}_{\dot{v}} \qquad m_z = m - \overset{\circ}{Z}_{\dot{w}} \tag{1}$$

where $\overset{\circ}{X}_{\dot{u}}$, $\overset{\circ}{Y}_{\dot{v}}$, $\overset{\circ}{Z}_{\dot{w}}$ are the gas mass terms for X, Y and Z axes respectively; whereas the apparent moments of inertia will be:

$$J_x = I_x - \overset{\circ}{L}_{\dot{p}} \qquad J_y = I_y - \overset{\circ}{M}_{\dot{q}} \qquad J_z = I_z - \overset{\circ}{N}_{\dot{r}} \tag{2}$$

with $\overset{\circ}{L}_{\dot{p}}$, $\overset{\circ}{M}_{\dot{q}}$, $\overset{\circ}{N}_{\dot{r}}$ gas inertia terms respectively about X, Y and Z axes. In the same way the apparent products of inertia can be computed as:

$$\begin{aligned} J_{xy} &= I_{xy} + \overset{\circ}{L}_{\dot{q}} \equiv I_{xy} + \overset{\circ}{M}_{\dot{p}} \\ J_{xz} &= I_{xz} + \overset{\circ}{N}_{\dot{p}} \equiv I_{xz} + \overset{\circ}{L}_{\dot{r}} \\ J_{yz} &= I_{yz} + \overset{\circ}{M}_{\dot{r}} \equiv I_{yz} + \overset{\circ}{N}_{\dot{q}} \end{aligned} \tag{3}$$

with $J_{xy} = J_{yz} = 0$ for the symmetry of the airship about the XZ plane and $J_{xz} = 0$ because XYZ are main inertia axes.

The 6 DOF equations of motion with the assumptions mentioned above may be developed by implementing Newton's second law of motion for each degree of freedom in turn. The force equations may therefore be written as:

Axial force

$$m_x\dot{u} - \overset{\circ}{X}_{\dot{q}}\,\dot{q} + m_z qw - m_y rv = \\ = F_{Xa} + F_{Xb} + F_{Xg} + F_{Xpr} \tag{4}$$

Side force

$$m_y\dot{v} - \overset{\circ}{Y}_{\dot{p}}\,\dot{p} - \overset{\circ}{Y}_{\dot{r}}\,\dot{r} + m_x ru - m_z pw = \\ = F_{Ya} + F_{Yb} + F_{Yg} + F_{Ypr} \tag{5}$$

Normal force

$$m_z\dot{w} - \overset{\circ}{Z}_{\dot{q}}\,\dot{q} + m_y pv - m_x qu = \\ = F_{Za} + F_{Zb} + F_{Zg} + F_{Zpr} \tag{6}$$

The corresponding moment equations will be:

Rolling moment

$$J_x\dot{p} - \left(J_y - J_z\right)qr - J_{xz}\left(\dot{r} + pq\right) - \overset{\circ}{L}_{\dot{v}}\,\dot{v} = \\ = L_a + L_b + L_{pr} \tag{7}$$

Pitching moment

$$J_y\dot{q} + \left(J_x - J_z\right)pr - J_{xz}\left(r^2 - p^2\right) - \overset{\circ}{M}_{\dot{u}}\,\dot{u} - \overset{\circ}{M}_{\dot{w}}\,\dot{w} = \\ = M_a + M_b + M_{pr} \tag{8}$$

Yawing moment

$$J_z\dot{r} - \left(J_x - J_y\right)pq - J_{xz}\left(\dot{p} - qr\right) - \overset{\circ}{N}_{\dot{v}}\,\dot{v} = \\ = N_a + N_b + N_{pr} \tag{9}$$

where terms on the right hand side of the six equations are components of force or moment respectively due to *a*erodynamic effects, static *b*uoyancy, *g*ravitational force and *pr*opulsion.

The aerodynamic force and moment components may be mathematically expressed in the usual dimensional derivative notation as functions of the perturbation variables *u*, *v*, *w*, *p*, *q* and *r*. For example the axial aerodynamic force can be written as:

$$F_{X_a} = F_{X_e} + \overset{\circ}{F}_{X_u}\,u + \overset{\circ}{F}_{X_v}\,v + \overset{\circ}{F}_{X_w}\,w + \overset{\circ}{F}_{X_p}\,p + \overset{\circ}{F}_{X_q}\,q + \overset{\circ}{F}_{X_r}\,r \tag{10}$$

where F_{X_e} is the trim equilibrium component of axial aerodynamic force and the remaining terms are dynamic terms present only during a perturbation. Whereas, in this dynamic model the aerodynamic forces and moments are expressed as:

$$\begin{aligned} F_{X_a} &= C_{F_x}\cdot 0.5\rho U^2 V^{2/3} \\ F_{Y_a} &= C_{F_y}\cdot 0.5\rho U^2 V^{2/3} \\ F_{Z_a} &= C_{F_z}\cdot 0.5\rho U^2 V^{2/3} \\ L_a &= C_L\cdot 0.5\rho U^2 V^{2/3} D \\ M_a &= C_M\cdot 0.5\rho U^2 V^{2/3} l \\ N_a &= C_N\cdot 0.5\rho U^2 V^{2/3} D \end{aligned} \tag{11}$$

where U is the free-stream airspeed, V is the airship model volume, D is the hull diameter and l is the reference length of the wet surface. The aerodynamic coefficients ($C_{F_x}, C_{F_y}, C_{F_z}, C_L, C_M, C_N$) are provided by 6 look-up tables estimated at different Reynolds numbers, in particular at *2 m/s*, *4 m/s*, *8 m/s* and *20 m/s*. The computation was performed by NSAERO, a finite volume multi-block computing code, which solves the Navier-Stokes equations including also the viscous effect[9]. The no perfect symmetry of the vehicle (because of the arms sustaining the propellers) relative to the XZ and XY planes, imposes the aerodynamic coefficient determination for positive and negative α and β ($-90° \le \alpha \le +90°$ and $-180° \le \beta \le +180°$).

The gravitational and buoyancy forces are static forces that produce components of force and moment through attitude perturbation (φ, ϑ, ψ) of the airship. The resulting expressions will be:

$$\begin{aligned} F_{x_b} + F_{x_g} &= -\left(mg - B\right)\sin\vartheta \\ F_{y_b} + F_{x_g} &= \left(mg - B\right)\sin\varphi\cos\vartheta \\ F_{z_b} + F_{z_g} &= \left(mg - B\right)\cos\varphi\cos\vartheta \\ L_b &= -Bb_z\sin\varphi\cos\vartheta \\ M_b &= -Bb_z\sin\vartheta - Bb_x\cos\varphi\cos\vartheta \\ N_b &= +Bb_x\sin\varphi\cos\vartheta \end{aligned} \tag{12}$$

where b_x and b_z are the coordinates of the CB relative to CG. The total buoyancy is:

$$B = V_b\,\Lambda_{air}\left(1 - \varepsilon_{He}\right) \tag{13}$$

where Λ_{air} is the specific weight of the ambient atmosphere, ε_{He} is the ratio between air and helium specific weight and V_b is their volume which will be some fraction δ of the hull volume. With the hypothesis of pressure and temperature kept constant inside the hulls, the value of buoyancy does not vary up to the *plenitude altitude*. Moreover, the airship can exceed this altitude and reach a maximum pression height losing progressively helium. The leakage of gas

causes also a loss of buoyancy and this force diminishes proportionally to the air specific weight:

$$B = \delta V \Lambda_{air} \frac{p_a}{p_{a_0}} \frac{T_{K_0}}{T_K} \left(1 - \varepsilon_{He}\right) \tag{14}$$

The dynamic model of the Nautilus unmanned airship takes also in account the variation of the CB position relative to the altitude: the coordinates b_x and b_z are provided at each time step of the simulation by two look-up tables as function of the actual and the plenitude altitude. The lateral shift of the buoyancy is not modeled: as a matter of fact when a bank angle occurs, an automatic valve closes the duct connecting the hulls and does not allow the air to flow from the inferior to superior ballonet.

The propulsion terms are introduced in the equations of motion modelling the thrust of each propeller and computing the components of force and moment relative to the airship CG reference frame. The first *Rénard formula*[10] is used to express the thrust for forward propellers:

$$T_{fw} = \tau_{fw} \rho_{air} \omega_{fw}^2 R_{fw}^4 \tag{15}$$

and vertical propellers:

$$T_{vt} = \tau_{vt} \rho_{air} \omega_{vt}^2 R_{vt}^4 \tag{16}$$

where R_{fw}, R_{vt} are the radii and ω_{fw}, ω_{vt} the pulsations of forward and vertical propellers respectively. The multiplicative terms τ_{fw} and τ_{vt} are provided by interpolating graphs that are functions of the blade mortise angle and the functioning point:

$$\eta_{fw} = U \Big/ \left(\omega_{fw} R_{fw}\right) \tag{17}$$

$$\eta_{vt} = U \Big/ \left(\omega_{vt} R_{vt}\right) \tag{18}$$

Acting on the two throttles, the RPM of forward and vertical propellers can be changed together with the magnitude of thrust vectors.

Two different control strategies can be selected to command the yaw attitude in forward flight: the asymmetric thrust and the over-steering. For example, in Figure 4 it is represented the asymmetric thrust control strategy for a right turn. The yaw moment around the Z body axis is obtained through a differential rotation of the forward propellers FFU and FFD relative to the rear propellers FRU and FRD, in addition the thrust of left propellers is greater than that of the right ones. The amount of the differential thrust between left and right propellers can be modified from a maximum of 50 % up to 0. In any case the resultant of side force remains to zero and the yaw moment is given by the following expression:

$$\begin{aligned} N_{pr} = &+ \left(T_{FFU} + T_{FFD}\right) \sin\gamma \cdot \left|x_{FFU}\right| + \\ &+ \left(T_{FRU} + T_{FRD}\right) \sin\left|-\gamma\right| \cdot \left|x_{FRU}\right| + \\ &+ 2\left(T_{FFD} - T_{FFU}\right) \cos\gamma \cdot \left|x_{FFD}\right| \end{aligned} \tag{19}$$

where $T_{FFD} = T_{FRU}$, $T_{FFU} = T_{FRD}$, γ is the rotation angle of each propeller and *x,y,z* are the coordinates of the propellers position vector in the CG reference frame. The yaw moment is always coupled to a roll moment due to the asymmetric placement of the forward propellers on the central plane. The undesired roll moment is given by the expression:

$$\begin{aligned} L_{pr} = &- \left(T_{FFD} - T_{FRD}\right) \sin\left|\gamma\right| \cdot \left|z_{FFD}\right| + \\ &- \left(T_{FRU} - T_{FFU}\right) \sin\left|\gamma\right| \cdot \left|z_{FFU}\right| \end{aligned} \tag{20}$$

and it has to be tackled acting on the roll command.

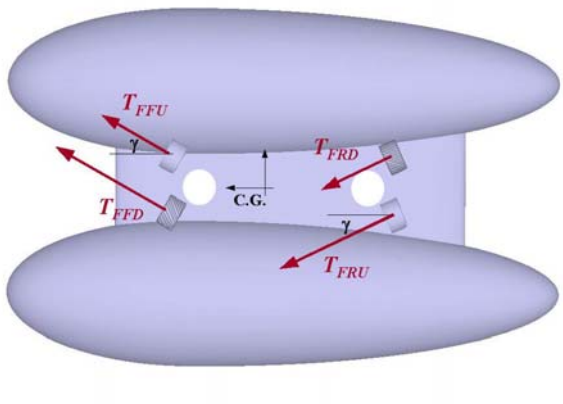

Figure 4. The asymmetric thrust control

To overcome this undesired rolling effect, the over-steering control strategy is designed and modeled in the flight simulator. As it can be seen in Figure 5, in order to perform the same right turn, only the rear fans FRU and FRD are rotated concordantly without a differential thrust. The resulting yaw moment is:

$$N_{pr} = +\left(T_{FRU} + T_{FRD}\right) \sin\gamma \cdot \left|x_{FRU}\right| \tag{21}$$

where $T_{FRU} = T_{FRD}$ and the pilot does not have to act on the roll command because the roll moment remains to zero. As drawback, this kind of control performs less efficient maneuvers because of the absence of differential thrust.

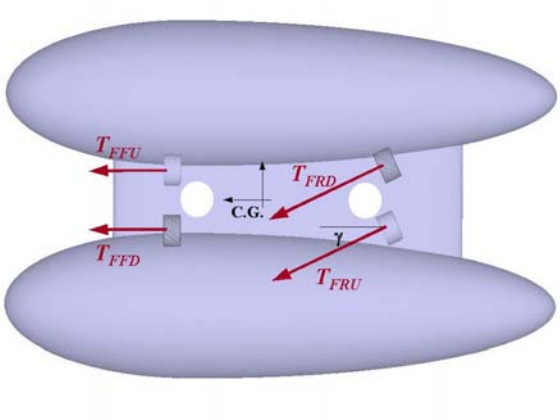

Figure 5. The over-steering control

The lateral command channel is designed to produce a roll moment through the cross differential rotation of the upper propellers (FFU and FRU) relative to the lower ones (FFD and FRD). The total roll moment generated is given by:

$$L_{pr} = +\left(T_{FFU} + T_{FRU}\right)\sin\gamma \cdot \left|z_{FFU}\right| + \\ +\left(T_{FFD} + T_{FRD}\right)\sin\left|-\gamma\right| \cdot \left|z_{FFD}\right| \tag{22}$$

with $T_{FFU} = T_{FFD} = T_{FRU} = T_{FRD}$.

Finally, the longitudinal command makes use of the differential thrust between upper (FFU and FRU) and lower (FFD and FRD) forward propellers and aft (FVA) and fore (FVF) vertical propellers. The resulting pitching moment is given by:

$$M_{pr} = +\left(T_{FFD} + T_{FRD}\right)\left|z_{FFD}\right| - \left(T_{FFU} + T_{FRU}\right)\left|z_{FFU}\right| + \\ +T_{FVA}\left|x_{FVA}\right| - T_{FVF}\left|x_{FVF}\right| \tag{23}$$

with $T_{FFD} = T_{FRD}$ and $T_{FFU} = T_{FRU}$.

These control strategies, together with *ad hoc* transfer functions on the primary command systems, satisfy the basilar requirements of a CAS for roll, pitch and yaw rate. Chosen the desired control strategy, the equations of motion from (4) to (9) are integrated step by step together with other two sets of mathematical expressions: the kinematic and the navigation equations[11]. As it can be noticed, the equations of motion are nonlinear ordinary differential equations with time varying coefficients. In fact, the apparent mass and inertia terms change as functions of the altitude, since they are computed relative to the CB of the airship.

5. Dynamic Characteristics

A subroutine to trim and linearize dynamic models is adapted and used to produce the following results. The longitudinal-dynamics system matrix A_{lon} for the Nautilus unmanned airship in straight and level flight at *500 m* and *10 m/s* is given in Table 1. The four states U, α, ϑ and q give rise to two complex-conjugate pairs of eigenvalues, which correspond to two oscillatory modes. The periods of these modes are separated by three order of magnitude ($T_{sp} = 16.3\,s$, $T_{ph} = 6636\,s$), so that they are easily identifiable as the *short period* and *phugoid* modes. The first couple of eigenvalues is referred to the unstable short period due to the intrinsic instability of the fuse architecture. Whereas the second couple is relative to the phugoid mode: it is well damped and its period is so long that the pilot would have no difficulty in damping out a phugoid oscillation.

$$A_{lon} = \begin{array}{c} \begin{matrix} U & \alpha & \theta & q \end{matrix} \\ \begin{bmatrix} -4.44E-3 & -4.60E-2 & -1.49E-1 & -7.97E-1 \\ 7.63E-6 & -7.21E-3 & 0 & 0 \\ 0 & 0 & 0 & 1 \\ 3.31E-3 & 7.58E-2 & -1.46E-1 & 0 \end{bmatrix} \end{array}$$

<u>*Short-Period mode*</u>

$+0.00162 \pm 0.386i \quad \rightarrow T_{sp} = 16.3\,s,\ \zeta_{sp} = 0.0042$

<u>*Phugoid mode*</u>

$-0.00745 \pm 0.00092i \quad \rightarrow T_{ph} = 6636\,s,\ \zeta_{ph} = 0.992$

Table 1. Longitudinal dynamic characteristics

The matrix A_{lat} for the lateral-directional dynamics of the airship model in the same flight condition is given in Table 2. The four lateral states β, ϕ, p and r give rise to two real eigenvalues and a complex-conjugate pair. The first mode is unstable and involves the roll rate producing a pendulum oscillation in roll: it is the *oscillatory roll* mode and its period is quite long ($T_{or} = 13.4\,s$). The second mode is the *yaw subsidence* mode and is a stable exponential mode distinguished by a very long time constant ($\tau_y = 1.46E+8\,s$). The third mode is also a simply stable exponential mode and involves the sideslip angle: it is the *sideslip subsidence* mode and its time constant ($\tau_s = 32.2\,s$) indicates a poor response to yaw maneuvers.

$$A_{lat} = \begin{array}{c} \begin{matrix} \beta & \phi & p & r \end{matrix} \\ \begin{bmatrix} -1.95E-1 & 0 & 8.74E-3 & 0 \\ 0 & 0 & 1 & -8.74E-3 \\ 2.20E-4 & -2.21E-1 & 0 & 0 \\ -8.72E-5 & -2.20E-2 & 0 & 0 \end{bmatrix} \end{array}$$

Oscillatory Roll mode

$+0.000000726 \pm 0.47i \;\rightarrow T_{or} = 13.4\,s$, ζ_{or} = -1.55E-6

Yaw subsidence mode

$-4.29E-8 \;\rightarrow \tau_y = 1.46E+8\,s$

Sideslip subsidence mode

$-0.195 \;\rightarrow \tau_s = 32.2\,s$

Table 2. Lateral-Directional dynamic characteristics

These dynamic characteristics are quite peculiar and point out the strong dynamic instability of the airship: small perturbations can excite the two longitudinal and lateral unstable modes contemporaneously making the airship uncontrollable.

6. Simulator Characteristics

The 6 DOF nonlinear airship model described in section 4 is implemented by using the *Flight Dynamics and Control* (FDC) toolbox[12] which is a graphical software environment within Matlab/Simulink. This toolbox is flexible and powerful enough to allow the implementation of different vehicle dynamic models and the design of several control architectures for research tasks. The general scheme of the simulation environment is shown in Figure 6 with the main blocks concerning airship dynamics, actuator transfer functions, pilot actions, control devices (hovering and forward flight, climb and descent) and different display options (i.e. vertical propellers throttle).

The airship dynamic model is flown through two throttles and a joystick with a manual switch linked (*hardware-in-the-loop*) to the Simulink environment for real time simulations. The first throttle acts on the RPM of the four forward propellers whereas the second one controls the RPM of the two vertical axes propellers. Furthermore the three-DOF joystick allows to maneuver the airship as described in detail in section 3. However, pre-loading of command histories is also possible in order to compare different simulation scenarios with respect to the same maneuver.

Finally, for graphic display and pilot interaction the dynamic model is interfaced with the *Aviator Visual Design Simulator* (AVDS) simulation package[13] as shown in Figure 7.

7. Flight Simulations

Different maneuvers have been accomplished in order to test the flight simulator of the Nautilus unmanned airship model. In Figures 8 and 9 it is shown the trend of some aerodynamic variables during an *ad hoc* maneuver realized to emphasize the lateral modes. In fact, the pilot acts on the yaw command in order to excite lateral-directional modes. As it can be seen in the last plot of Figure 8, the yaw angle tends to increase indefinitely according to the large time costant of the *yaw subsidence* mode and the pilot has to tackle this effect. The sideslip angle trend (first plot of Figure 9) shows a low response according to the *sideslip subsidence* mode. Due to the coupling between lateral and directional dynamics, the unstable *oscillatory roll* mode is excited as it can be seen from the time histories of the bank angle (second plot of Figure 8) and roll rate (second plot of Figure 9). In addition the pilot has to act constantly on the longitudinal command in order to handle the unstable *short period* mode.

8. Conclusions

In this paper a simulation tool for the Nautilus new concept unmanned airship has been presented. The simulation package provides a customized yet flexible environment for analyzing different research issues and represents an intermediate step between the design and the final manufacturing of the airship and its control system. At present the airship design is focused on the subsystem test and assembling. The schedule foresees the conclusion of the detailed design within 2003, the realization of the first prototype in 2004 and first flight tests in summer 2004.

The airship model presents a longitudinal and lateral intrinsic instability due to the fuse architecture. Flight tests performed on the airship flight simulator seem to be promising: the airship is sufficiently maneuverable even if in a open-loop configuration, namely without automatic control systems.

In the future, automatic control systems (such as CAS, SAS and autopilots) will be designed and implemented on-board to improve dynamic characteristics and achieve desired flying qualities without demanding an excessive workload to the pilot.

References

1. Elfes A., Bueno S.S., Bergerman M., Ramos J.Jr.G., "A Semi-Autonomous Robotic Airship for Environmental Monitoring Missions", *Proceedings of the 1998 IEEE International Conference on Robotics & Automation*, Leuven, Belgium, May 1998, pp. 3449-3455.
2. Zaugg D.A., Arnold D.V., Jensen M.A., "Ocean Surface and Landside Probing with a Scanning Radar Altimeter", *Proceedings of the 2000 International Geoscience and Remote Sensing Symposium,* vol. 1, 2000, pp. 120-120.

3. Hain J.H.W., "Lighter-than-air Platforms (Blims and Aerostats) for Oceanographic and Atmospheric Research and Monitoring", *Proceedings of the Oceans 2000 MTS IEEE Conference and Exhibition*, vol. 3, 2000, pp. 1933-1936.
4. Valera J.L., "Some Remarks on the Conceptual Design of a Heavy Lift Cargo Transporter", *Proceeding of the 14th AIAA Ligther-Than-Air Technical Committee Convention & Exhibition*, Akron, OH, July 2001.
5. Khoury G.A., Gillett J.D., "Airship Technology", *Cambridge University Press*, 1999.
6. Azinheira J.R., Carneiro de Paiva E., Ramos J.Jr.G., Bueno S.S., Bergerman M., Gomes S.B.V., "Extended Dynamic Model For Aurora Robotic Airship", *Proceeding of the 14th AIAA Ligther-Than-Air Technical Committee Convention & Exhibition*, Akron, OH, July 2001.
7. Varella Gomes S.B., Ramos J.Jr.G., "Airship Dynamic Modelling for Autonomous Operation", *Proceedings of the 1998 IEEE International Conference on Robotics & Automation"*, Leuven, Belgium, May 1998, pp. 3462-3467.
8. Carneiro de Paiva E., Bueno S.S., Gomes S.B.V., Ramos J.Jr.G., Bergermann M., "A Control System Development Environment for AURORA's Semi Autonomous Robotic Airship", *Proceedings of the 1999 IEEE International Conference on Robotics & Automation*, Detroit, MI, May 1999, pp. 2328-2335.
9. Battipede M., Gili P.A., Massotti L., Vercesi P., "Design Characteristics of a Non Conventional Thrust-Vectored Airship", *Proceedings of the 2003 UAV International Technical Conference & Exhibition,* Paris, France, June 2003.
10. Lausetti A., Filippi F., "Elementi di Meccanica del Volo", *Levrotto&Bella*, Turin, I, 1955, pp. 61-88.
11 Stevens B. L., Lewis F.L., "Aircraft Control and Simulation", *John Wiley & Sons, Inc.*, New York, 1992, pp. 80-82.
12. Rauw M.O., "*FDC 1.2: A Simulink Toolbox for Flight Dynamics and Control Analysis*", Delft University of Technology, The Netherlands, 1998.
13."*Aviator Visual Design Simulator (AVDS) – User Manual*", Rassmussen Simulation Techn., Ltd., Oct. 2000.

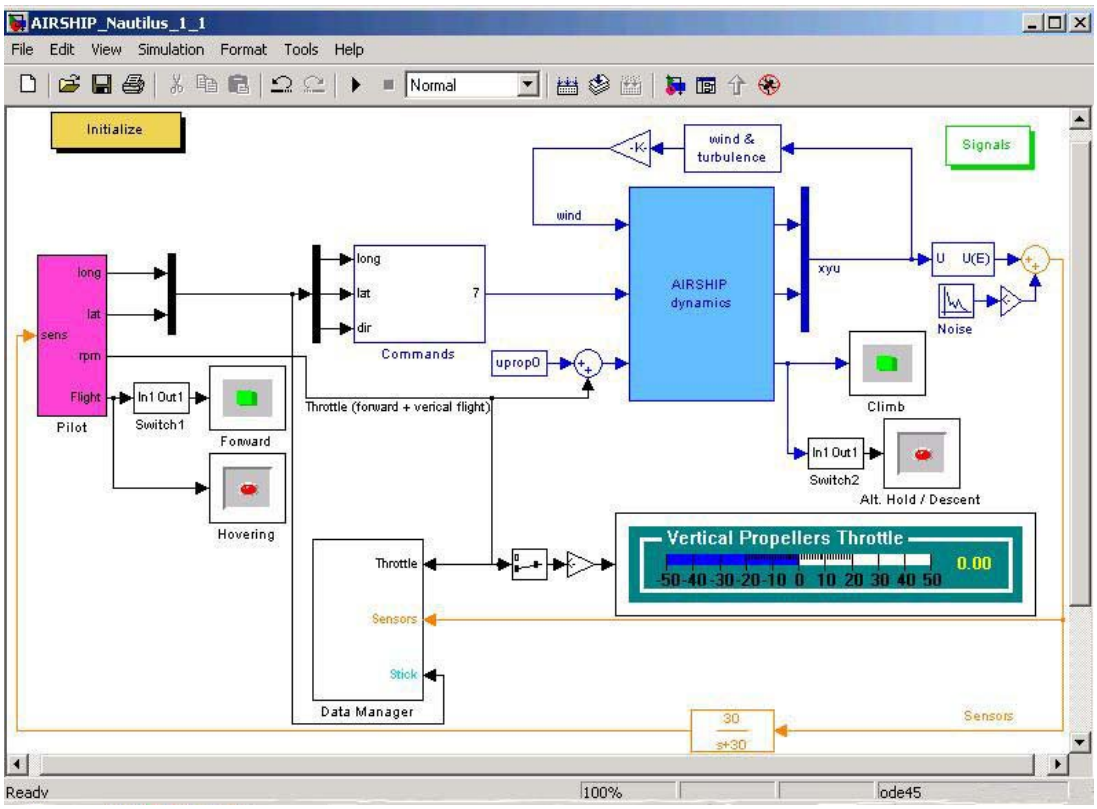

Figure 6. SIMULINK Highest Level Typical Scheme for the Nautilus unmanned airship model

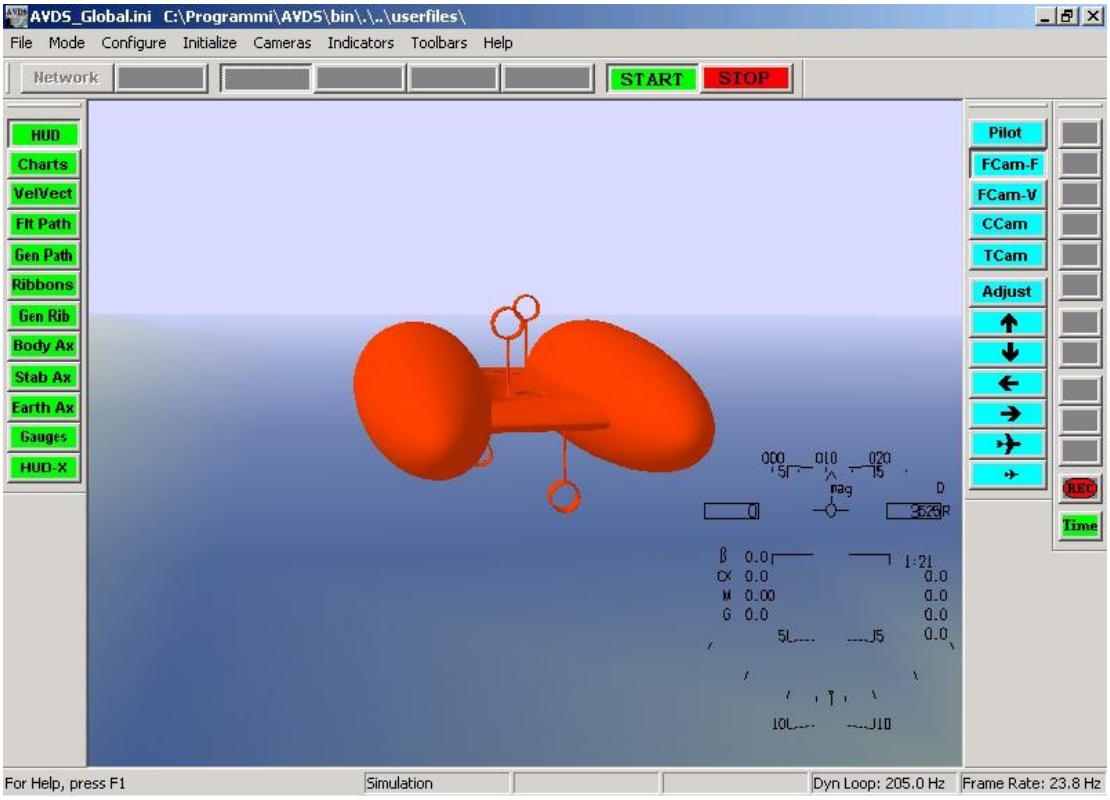

Figure 7. AVDS/SIMULINK Graphic Environment of the Nautilus unmanned airship model

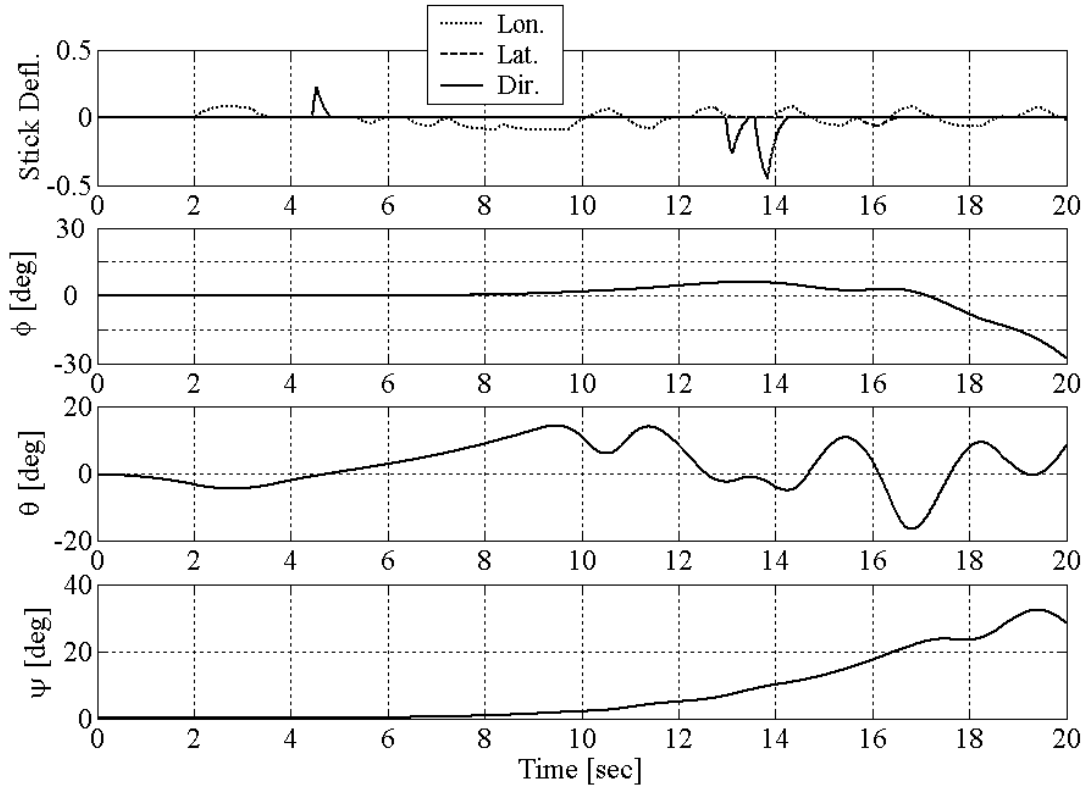

Figure 8. Stick deflections and Euler angles

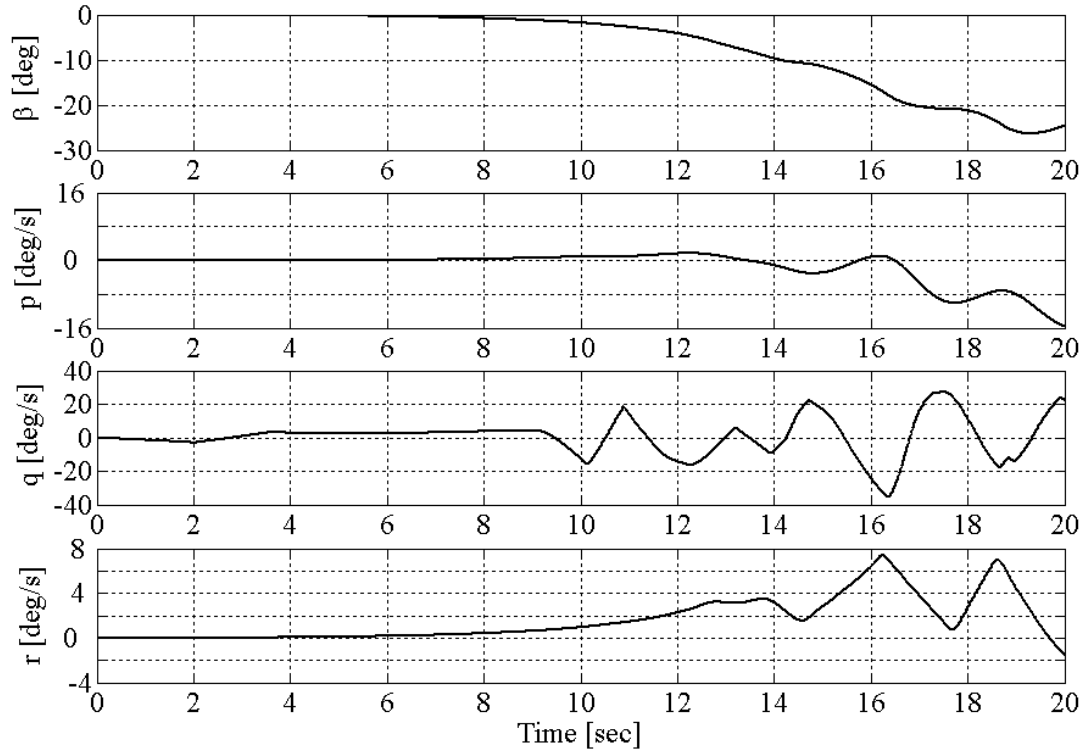

Figure 9. Sideslip angle and angular rates